Environmental Science & Technology

Article

pubs.acs.org/est

Role of Organic Carbon in Heterogeneous Reaction of NO_2 with Soot

Chong Han, Yongchun Liu, and Hong He*

Research Center for Eco-Environmental Sciences, Chinese Academy of Sciences, Beijing, 100085, China

Ⓢ *Supporting Information*

ABSTRACT: A large uncertainty among the reported uptake coefficients of NO_2 on soot highlights the importance of the composition of soot in this reaction. Soot samples with different fractions of organic carbon (OC) were prepared by combusting *n*-hexane under controlled conditions. The heterogeneous reaction of NO_2 on soot was investigated using a flow tube reactor at ambient pressure. The soot with the highest fuel/oxygen ratio showed the largest uptake coefficient ($\gamma_{initial}$) of NO_2 and yield of HONO (y_{HONO}). Compared to fresh soot samples, preheated samples exhibited a great decrease in uptake coefficient of NO_2 and HONO yield due to the removal of OC from soot. Ozonized soot also showed a lower reactivity toward NO_2 than fresh soot, which can be ascribed to the consumption of OC with a reduced state (OC_R). A linear dependence of the NO_2 uptake coefficient and yields of HONO and NO on the OC_R content of the soot was established, with $\gamma_{initial}(NO_2) = (1.54 \pm 1.39) \times 10^{-6} + (1.96 \pm 0.35) \times 10^{-7} \times OC_R$, $y_{HONO} = (11.6 \pm 16.1) + (1.3 \pm 0.40) \times OC_R$, and $y_{NO} = (13.1 \pm 1.9) - (0.2 \pm 0.05) \times OC_R$, respectively.

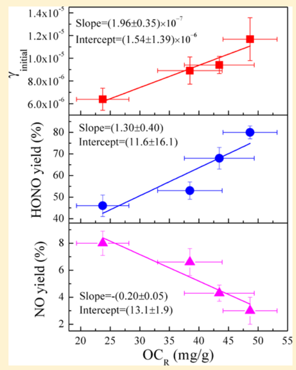

1. INTRODUCTION

Soot particles, which originate from the incomplete combustion of fossil fuels and biomass, are primarily composed of elemental carbon (EC) with variable fractions of organic carbon (OC).[1,2] It has been widely recognized that soot particles in the atmosphere are responsible for global and regional climate change. For example, the contribution of soot to global warming is estimated to be second only to that of CO_2.[3] Soot has an important impact on the global radiative balance directly by absorbing solar energy and indirectly by acting as cloud condensation nuclei (CCN) and ice nuclei (CN).[4,5] It is also reported that soot is responsible for the increase in droughts or floods in China over the past 20 years and haze formation over Southern Asia.[5−7] In addition, soot also poses a health risk by causing and enhancing respiratory, cardiovascular, and allergic diseases.[8]

Soot particles with a large specific surface area may change the atmospheric composition through reacting with active species such as OH, O_3, NO_2, NO_3, N_2O_5, HNO_3, and H_2SO_4.[9−18] In particular, chemical interactions between soot and NO_2 have attracted considerable attention in the past years since they may play an important role in the HONO source and HO_x balance in the atmosphere,[12−14,19−24] thus affecting the oxidizing capacity of the atmosphere. Up to now, several studies have measured the uptake coefficient (γ) of NO_2 on different types of soot including fuel combustion soot such as *n*-hexane,[13,20,21,23] decane,[13,21] diesel fuel,[19] and toluene,[19,20] commercially available soot Degussa FW2 and Printex,[19] and spark discharge soot from graphite electrodes.[22,24] However, the reported values of γ varied from 10^{-1} to 10^{-8} dependent on the origins of soot.[12−14,19−24] Even though the specific surface area of soot samples was considered, the reported γ also varied from 10^{-4} to 10^{-8}.[21] On the other hand, many studies found that NO_2 can be transformed to HONO and NO,[12−14,19−22] whereas Prince et al. demonstrated that NO_2 was only adsorbed on soot without any accompanying chemical reaction.[23] Thus, the yield of HONO is also highly variable from 0 to 100%. These controversial results imply that the composition of soot may be a crucial factor for the differences in reactivity of soot. Stadler and Rossi found that a lower fuel/air ratio of the diffusion flame results in lower hydrogen content and higher oxygen content of soot, and lower reactivity for the reduction of NO_2 to HONO.[13]

Additionally, it has been observed that organic species (C−H) on the soot surface can be consumed during the uptake of NO_2 and formation of HONO and NO.[12−14,25] Formation of nitrogen-containing species such as $R{-}NO_2$, $R{-}ONO_2$, and R−ONO was also observed through infrared spectroscopy.[25−29] The OC component in soot was mainly composed of highly functionalized carbonaceous compounds, such as saturated and unsaturated hydrocarbons, alkanoic acids, substituted aromatics, alcohols, ketones, polycyclic aromatic hydrocarbons, and their derivatives.[30] Thus, these results posed a new question concerning how the reactivity of soot to NO_2 depends on the soot composition. To the best of our knowledge, however, this quantitative relationship among the NO_2 uptake coefficients, yields of HONO and NO, and OC content of soot has not been established yet.

In this study, soot samples with different fractions of OC were generated through combusting *n*-hexane under well-controlled combustion conditions. The heterogeneous reaction of soot with NO_2 was investigated in a flow tube reactor coupled to a NOx analyzer at ambient pressure. Fresh,

Received: November 2, 2012
Revised: March 4, 2013
Accepted: March 7, 2013
Published: March 7, 2013

   dx.doi.org/10.1021/es304468n | Environ. Sci. Technol. 2013, 47, 3174−3181

preheated and ozonized soot samples were examined to assess the role of OC in the reactivity of soot to NO_2. A quantitative relationship among the NO_2 uptake coefficients, yields of HONO and NO, and content of OC in a reduced state was found. These results will increase the understanding of the differences in the reported reactivities among soot samples and help to assess the atmospheric HONO contribution of soot dependence on OC fractions.

2. EXPERIMENTAL SECTION

Soot Production. Soot particles were produced by burning *n*-hexane (AR, Sinopharm Chemical Reagent Lo., Ltd.) in a coflow diffusion burner, which has been described elsewhere in detail.[31] This coflow burner basically consisted of a diffusion flame that was maintained in an airflow, which was controlled by mass flow meters to regulate the fuel/oxygen ratio. The fuel was fed by a cotton wick extending into the liquid fuel reservoir. The airflow with a range of O_2 content from 21.5 to 32.5% was a mixture of high purity oxygen and nitrogen. The fuel/oxygen ratio was expressed as the molar ratio of the consumed fuel to the introduced oxygen during the combustion process. The fuel/oxygen ratio was in the range of 0.100−0.180. Soot samples were collected at the exit of the burner on the inner walls of a quartz tube (20 cm length, 1.0 cm i.d.). The specific surface area of the soot was measured to be 52.0−56.0 m^2/g by nitrogen Brunauer−Emmett−Teller (BET) physisorption (Quantachrome Autosorb-1-C).

Flow Tube Reactor. The uptake experiments were performed in a horizontal cylindrical coated-wall flow tube reactor (34 cm length, 1.6 cm i.d.) which was similar to that used by Monge et al.[32] and is shown in Figure S1 of the Supporting Information. The experiments were maintained at 298 K by circulating water bath through the outer jacket of the flow tube reactor. High purity nitrogen was used as carrier gas, and the total flow rate introduced in the flow tube reactor was 930 mL min^{-1}, ensuring a laminar regime. NO_2 was introduced into the flow tube through a movable injector with 0.3 cm radius. During uptake experiments of NO_2 on soot, relative humidity was 7% that was measured by a hygrometer (Center 314). The NO_2 concentration was 160 ppb and the experiments were performed at ambient pressure. The NO_2 and NO concentrations were measured using a chemiluminescence analyzer (THERMO 42i) during the heterogeneous reaction of soot with NO_2. A denuder tube (10 cm × 0.6 cm i.d.) containing Na_2CO_3 was introduced between the exit of the flow tube reactor and the detector since HONO is detected as NO_2 by the analyzer.[32] NO and NO_2 together with HONO can be detected using a bypass tube, whereas only NO and NO_2 can be measured using this denuder because HONO is trapped from the gas stream by Na_2CO_3. Thus, the HONO concentration can be obtained as the difference between the detector signal without and with the carbonate denuder in the sampling line. No significant uptake of NO_2 and formation of HONO and NO were observed when 160 ppb NO_2 was introduced into the blank flow tube. Only 3% of the total NO_2 was trapped in the denuder, and this value has been considered in the calculation of the uptake coefficients and products yield.

Uptake Coefficient. The kinetic behavior of the NO_2 can be well described by assuming a pseudo first-order reaction with respect to the gas-phase NO_2 concentration. The first-order rate constant (k_{obs}) is related to the geometric uptake coefficient (γ) using eq 1:

$$\frac{d}{dt}\ln\frac{C_0}{C_i} = k_{obs} = \frac{\gamma\langle c\rangle}{2r_{tube}} \quad (1)$$

where r_{tube}, t and $\langle c\rangle$ are the flow tube radius, the exposure time, and the NO_2 average molecular velocity, respectively. C_0 and C_i is the NO_2 concentration at $t = 0$ and $t = i$, respectively. Because diffusion of NO_2 into underlying layers of the soot sample can take place, γ is dependent on sample mass and exhibits a linear increase in range of 0.3−2.0 mg. Therefore, the uptake coefficient normalized to the BET surface area (γ_{BET}) was calculated using eq 2:

$$\gamma_{BET} = \frac{S_{geom} \times \gamma_{geom}}{S_{BET} \times m_{soot}} \quad (2)$$

where S_{geom} is the geometric area of the flow tube reactor, S_{BET} is the BET surface area of soot, and m_{soot} is the soot mass.

If the loss of NO_2 at the soot surface is too rapid to be recovered with the NO_2 supply, a radial concentration gradient in the gas phase will be formed, which may cause diffusion limitations. Therefore, a correction for diffusion in the gas phase should be taken into account. Here, the Cooney-Kim-Davis (CKD) method was used to correct uptake coefficients,[33,34] which has been widely described in previous articles.[32,35,36] Initial uptake coefficients $\gamma_{initial}$ were determined by averaging the signal during the first 1.0 min.

3. RESULTS

OC Content of Soot Produced at Different Fuel/Oxygen Ratios. The OC content of soot produced with different fuel/oxygen ratios was measured using thermal gravimetric analysis. The content of condensed OC on soot in this study was directly measured to be in the range of 35−60 mg/g. As shown in Figure 1, the OC content showed an increase with increasing fuel/oxygen ratio. This can be well understood since a lower fuel/oxygen ratio should have higher combustion efficiency for fuels, thus leading to a lower amount of OC in soot samples. Thus, the difference in OC fractions may contribute to the varying reactivities of soot produced at different fuel/oxygen ratios.

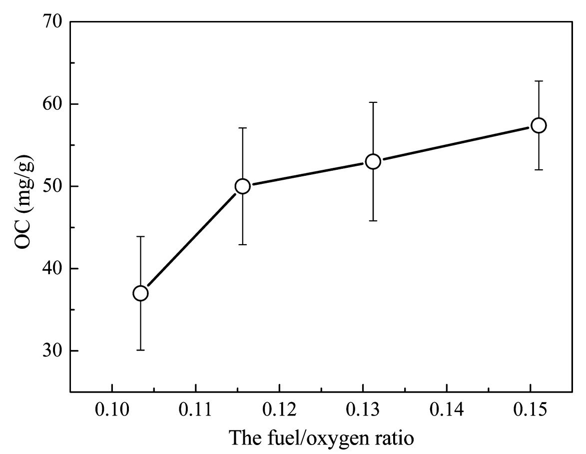

Figure 1. OC content of fresh soot with different fuel/oxygen ratios.

Reaction of NO_2 on Fresh Soot. As shown in Figure S2 of the Supporting Information, uptake of NO_2 and formation of HONO and NO were observed during heterogeneous reaction of soot with NO_2. The same experiments were also performed

dx.doi.org/10.1021/es304468n | Environ. Sci. Technol. 2013, 47, 3174−3181

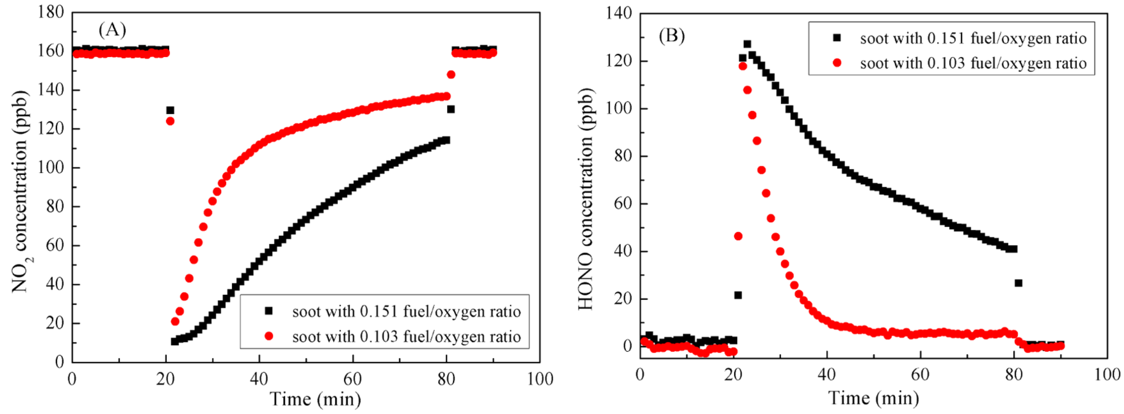

Figure 2. NO_2 uptake and HONO formation on soot produced at fuel/oxygen ratios of 0.151 and 0.103.

Table 1. $\gamma_{initial}$, HONO Yield, Integral Amount of HONO and NO Yield on Soot Produced at Different Fuel/Oxygen Ratios

fuel/oxygen ratio	$\gamma_{initial}$ (10^{-5})	HONO yield (%)	integral amount of HONO (molecules/mg within 1 h)	NO yield (%)
0.151	1.17 ± 0.29	80 ± 3	(1.01 ± 0.15) × 10^{17}	3.0 ± 1.0
0.131	0.94 ± 0.08	68 ± 5	(0.75 ± 0.16) × 10^{17}	4.3 ± 0.6
0.116	0.89 ± 0.12	53 ± 4	(0.38 ± 0.08) × 10^{17}	6.6 ± 1.0
0.103	0.64 ± 0.10	46 ± 5	(0.31 ± 0.08) × 10^{17}	8.0 ± 0.9

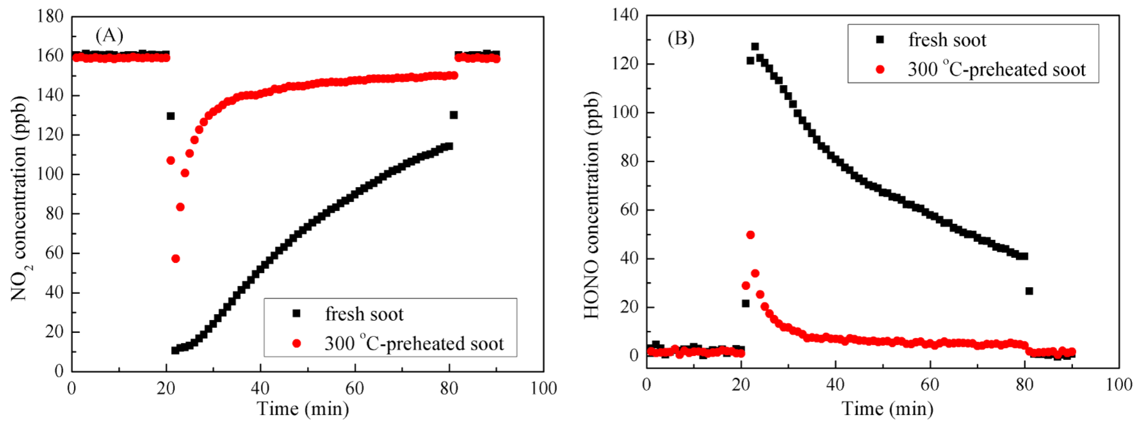

Figure 3. NO_2 uptake (A) and HONO formation (B) on fresh and 300 °C-preheated soot.

for soot samples produced at different fuel/oxygen ratios. As shown in Figure 2, soot produced at a 0.151 fuel/oxygen ratio exhibited slower deactivation rates of NO_2 uptake and HONO formation than soot generated at a 0.103 fuel/oxygen ratio. This indicates that the former contains more active sites toward NO_2 than the latter. Table 1 summarizes the NO_2 uptake coefficients, HONO yield, integral amount of HONO, and NO yield on soot produced at different fuel/oxygen ratios. The errors represent the standard deviations (σ) based on three independent experiments. Compared to those for soot produced at a 0.151 fuel/oxygen ratio, the initial uptake coefficients ($\gamma_{initial}$) for soot produced at 0.103 fuel/oxygen ratio decreased by 45%. The HONO yield for soot with 0.151 fuel/oxygen ratio was found to be 80%, whereas it decreased to less than 50% for soot with 0.103 fuel/oxygen ratio. The integral amount of HONO within 1 h decreased from (1.01 ± 0.15) × 10^{17} to (0.31 ± 0.08) × 10^{17} molecules/mg with fuel/oxygen ratio from 0.151 to 0.103. However, the NO yield exhibited an opposite trend with decreasing fuel/oxygen ratio. It was only 3% for soot with 0.151 fuel/oxygen ratio, and increased up to 8% for the soot with 0.103 fuel/oxygen ratio. These results confirmed that combustion conditions can significantly influence the reactivity of soot toward NO_2.

Changes in the functional groups on soot were also investigated using in situ ATR-IR spectra as detailed in the Supporting Information. As shown in Figure S3 of the Supporting Information, significant changes for several peaks were observed when the soot sample was exposed to 160 ppb NO_2. There were substantial losses in intensities for the bands at 3284 and 3058 cm^{-1}, which were assigned to the alkyne ≡C−H and aromatic Ar−H stretch,[25,37] respectively. A great increase in intensity of the bands at 1550, 1510, 1470, 1332, 1290, 1120, and 1054 cm^{-1} implies the formation of nitrogen-containing compounds such as $R-NO_2$ and $R-O-NO_2$.[25−29] Therefore, formation of nitro compounds can explain the fact that the total yields of HONO and NO were lower than 100% for all soot samples (Table 1).

Reaction of NO_2 on Preheated Soot. Soot is often described as a mixture of elemental carbon (EC) and organic carbon (OC).[1,2] The EC is mainly composed of a polyaromatic backbone, while the OC is composed of semivolatile compounds condensed onto EC. To investigate the role of OC in the reactivity of soot toward NO_2, we further examined

Table 2. Summaries of $\gamma_{initial}$, HONO Yield, Integral Amount of HONO and NO Yield on Fresh and Preheated Soot

types of soot	$\gamma_{initial}$ (10^{-5})	HONO yield (%)	integral amount of HONO (molecules/mg within 1 h)	NO yield (%)
fresh soot	1.17 ± 0.29	80 ± 3	(1.01 ± 0.15) × 10^{17}	3.0 ± 1.0
100 °C-preheated soot	0.85 ± 0.14	62 ± 1	(0.34 ± 0.02) × 10^{17}	4.9 ± 0.8
200 °C-preheated soot	0.27 ± 0.04	50 ± 5	(0.24 ± 0.05) × 10^{17}	8.3 ± 0.9
300 °C-preheated soot	0.18 ± 0.08	39 ± 5	(0.13 ± 0.02) × 10^{17}	20.7 ± 0.2
600 °C-preheated soot	0.16 ± 0.02	38 ± 3	(0.09 ± 0.01) × 10^{17}	22.1 ± 1.2

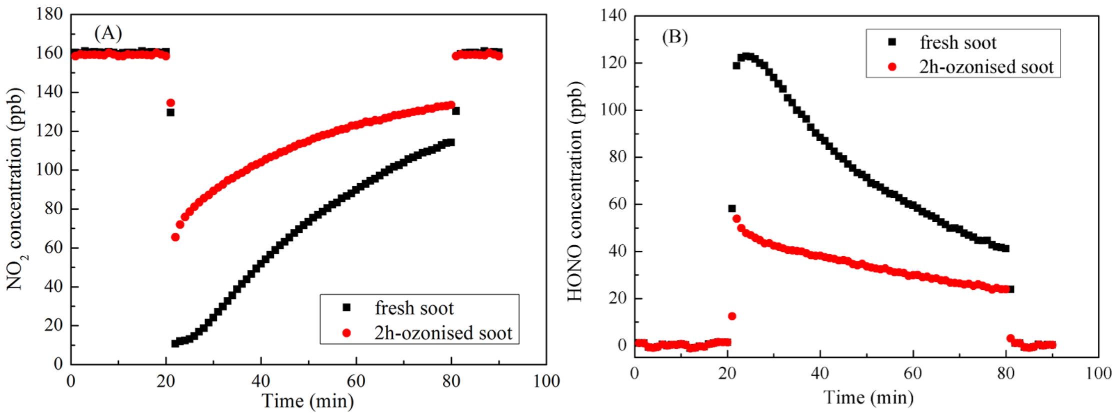

Figure 4. NO_2 uptake and HONO formation on fresh soot and soot oxidized by 100 ppb O_3.

Table 3. $\gamma_{initial}$, HONO Yield, Integral Amount of HONO and NO Yield on Fresh Soot and Soot Oxidized by 100 ppb O_3

types of soot	$\gamma_{initial}$ (10^{-5})	HONO yield (%)	integral amount of HONO (molecules/mg within 1 h)	NO yield (%)
fresh soot	1.17 ± 0.26	80 ± 3	(1.01 ± 0.15) × 10^{17}	3.0 ± 1.0
0.5h-ozonized soot	0.54 ± 0.02	76 ± 2	(0.92 ± 0.09) × 10^{17}	1.5 ± 0.4
1h-ozonized soot	0.25 ± 0.04	72 ± 6	(0.79 ± 0.08) × 10^{17}	1.4 ± 0.1
2h-ozonizedsoot	0.18 ± 0.04	64 ± 2	(0.51 ± 0.04) × 10^{17}	1.1 ± 0.1

the NO_2 uptake on the soot preheated at 300 °C in nitrogen as detailed in the Supporting Information. As shown in Figure 3, the preheated soot showed a smaller NO_2 initial uptake with a faster recovery rate than fresh soot. The HONO concentration for preheated soot also exhibited a smaller initial maximum followed by a faster decrease.

Compared with that for the fresh soot, the $\gamma_{initial}$ of soot preheated at 300 °C decreased from 1.17×10^{-5} to 0.18×10^{-5} (Table 2). Correspondingly, the HONO yield decreased from 80% to 39%, and the integral amount of HONO decreased from $(1.01 \pm 0.15) \times 10^{17}$ to $(0.13 \pm 0.02) \times 10^{17}$ molecules/mg, whereas the NO yield increased from 3.0% to 20.7%. The decreased $\gamma_{initial}$, HONO yield, and integral amount of HONO may be mainly ascribed to removal of active OC components. Previous studies have found that EC can also provide active sites for NO_2 adsorption, which subsequently decompose into NO and surface oxygen.[38] Therefore, the increase of NO yield is ascribed to more available EC in the soot skeleton when OC was removed at elevated temperature. To further completely remove OC and investigate the reactivity of EC toward NO_2, soot was also heated at 600 °C in nitrogen. Thus, experimental results for the 600 °C-preheated soot might represent the reactivity of EC toward NO_2. This means that the $\gamma_{initial}$, HONO yield, the integral amount of HONO, and NO yield for EC was $(0.16 \pm 0.02) \times 10^{-5}$ molecules/mg, (38 ± 3%), $(0.09 \pm 0.01) \times 10^{17}$ molecules/mg, and (22.1 ± 1.2%), respectively.

Reaction of NO_2 on Ozonized Soot. The effect of aging by O_3 was also investigated to confirm the role of reduction state in reactivity of soot toward NO_2 as detailed in the Supporting Information. Soot that had previously been exposed to 100 ppb O_3 was then exposed to 160 ppb NO_2. The deactivation of ozonized soot toward NO_2 is clearly observed (Figure 4). Ozonized soot exhibited a smaller uptake activity of NO_2 and lower HONO yield and the integral amount of HONO than the corresponding fresh soot. All of the $\gamma_{initial}$, HONO yield, the integral amount of HONO and NO yield exhibited an obvious decreasing trend with increasing ozonation time (Table 3). Compared to those for fresh soot, the decreasing amplitude of $\gamma_{initial}$, HONO yield, the integral amount of HONO and NO yield for 2h-ozonized soot was 85%, 20%, 50%, and 63%, respectively. This demonstrates that aging by O_3 can significantly decrease the reactivity of soot toward NO_2.

4. DISCUSSION

OC As Main Active Component. It is well-recognized that incomplete combustion can produce a broad range of organic compounds such as saturated and unsaturated hydrocarbons, polycyclic aromatic hydrocarbons, and partially oxidized organics, which can condense onto the soot surface.[2,14] The decrease in reactivity of preheated soot suggests that OC provides the main reactive sites to NO_2 (Figure 3). Through Soxhlet extraction using tetrahydrofuran as a solvent, Stadler and Rossi also demonstrated that the organic fraction that was condensed on the elemental carbon backbone structure of soot is active for NO_2 uptake and HONO production.[13] George et al. also observed significant NO_2 uptake and HONO formation on various model compounds such as benzophenone, catechol, perylene, anthracene, syringic acid, and their mixtures,[39] which may be produced during incomplete combustion of fuel. These

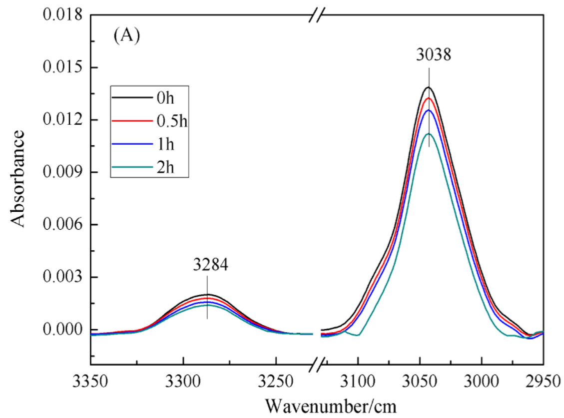

Figure 5. In situ ATR-IR spectra in the range of 3350−2950 cm^{-1} (A) and 1800−1500 cm^{-1} (B) for soot oxidized by 100 ppb O_3.

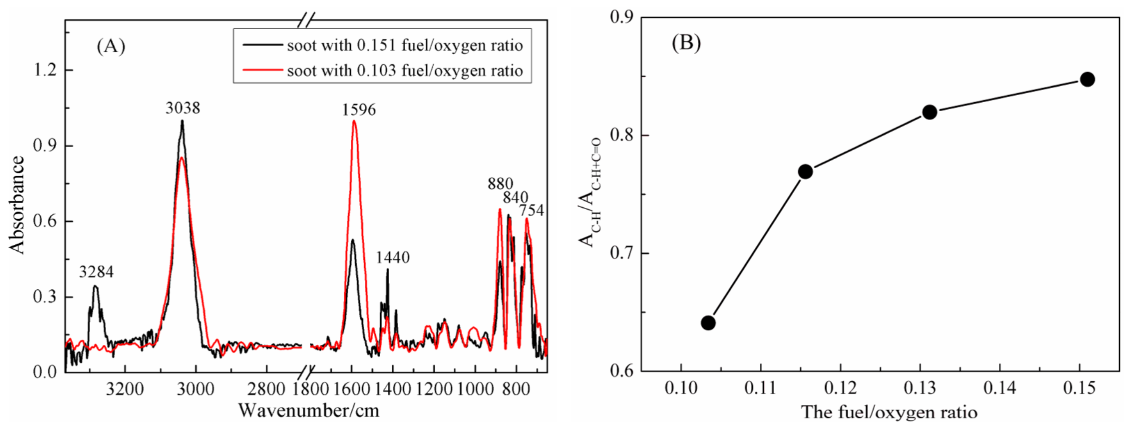

Figure 6. ATR-IR spectra for fresh soot with 0.151 and 0.103 fuel/oxygen ratio (A), Changes of the integrated areas ratio $A_{C-H}/A_{C-H+C=O}$ (the ratio of peak areas of all C−H groups to peak areas of all groups) (B).

results suggest that OC should be active sites toward NO_2. However, Khalizov et al. observed an increased reactivity of preheated soot compared with fresh soot using a low-pressure (1.5 Torr) flow tube reactor.[14] This may be ascribed to differences in the content and nature of OC on soot produced under different combustion conditions.

Once exposed to 100 ppb O_3 (Figure 5), the bands at 3284 and 3038 cm^{-1}, which were assigned to the stretching vibration of alkyne ≡C−H and aromatic C−H respectively, decreased noticeably. At the same time, a prominent increase in the intensity of the bands at 1714, 1685, and 1596 cm^{-1} indicates the formation of several oxygen-containing species such as carbonyl C═O. This demonstrates that OC_R was significantly consumed in reaction with O_3, thus leading to an increase in oxidation state of soot surface. Pryor and Lightsey have shown that HONO can be produced during the reaction of NO_2 with unsaturated hydrocarbons in the liquid phase with abstraction of the allylic hydrogen.[40] A similar mechanism may occur on soot since consumption of alkyne ≡C−H and aromatic C−H was also observed in the reaction of NO_2 with soot (in Figure S2 of the Supporting Information). Thus, ozonation, which involves the reaction of ozone with unsaturated carbon−carbon bonds, leads to a decrease in NO_2 uptake and HONO formation (in Figure 4) because loss of unsaturated C atoms will reduce the number of allylic H atoms. Soot may also contain several partially oxidized polyaromatic compounds with functionalities like OH, OCH_3, and so forth.[41] Arens et al. found significant amount of HONO when the hydroxy and methoxy aromatics were deposited on different substrates and exposed to NO_2 in humid air.[42] The ozone may also further oxidize the hydroxy and methoxy aromatics on soot, leading to the decrease in reactivity of soot to NO_2. These results suggest that OC_R should be the main active species toward NO_2. Through comparing Tables 2 and 3, it was found that the $\gamma_{initial}$ of NO_2 on the 2h-ozonized soot is very close to that of NO_2 on EC (preheated-600 °C soot). However, the HONO yield for the 2h-ozonized soot is higher than that for EC. This indicates that the remaining OC_R as well as the partially oxidized products from ozonation might be still active toward HONO formation. It should be noted that OC cannot be completely oxidized into CO_2 and H_2O by O_3, and the partially oxidized products should still be retained on the surface. Thus, ozonation treatment might not provide more EC sites for NO_2 decomposition. At the same time, O_3 can also lead to the partial oxidation of some bare EC,[43] and should reduce the active sites for reduction of NO_2 to NO. These factors should be the reason for the decreased yield of NO on the ozonized soot (Table 3).

Quantitative Analysis of Role of OC. According to the gaseous and surface products (Figures S1 and S2 of the Supporting Information), it can be confirmed that NO_2 was reduced to HONO, NO, and surface nitrogen-containing compounds. The ozonized soot also showed a lower reactivity toward NO_2 than fresh soot (Figure 4). These results demonstrate that the degree of reduction of the soot surface should have an important effect on the reactivity of soot toward

NO_2. Part A of Figure 6 compares the ATR-IR spectra of fresh soot with 0.151 and 0.103 fuel/oxygen ratios. For these two soot samples, there is little difference in the absorption band at 1440 cm^{-1} attributed to unsaturated CH_2 and the three bands in the range of 900−700 cm^{-1} assigned to the substitution modes of aromatic compounds.[25,37] Compared to the fresh soot with 0.151 fuel/oxygen ratio, however, the fresh soot with 0.103 fuel/oxygen ratio showed a stronger peak at 1596 cm^{-1} for carbonyl group bound to an aromatic ring and a weaker peaks at 3038 cm^{-1} for aromatic C−H.[25,37] The peak at 3284 cm^{-1} assigned to alkyne ≡C−H disappeared for soot with 0.103 fuel/oxygen ratio.[25,37] The integrated area ratio ($A_{C-H}/A_{C-H+C=O}$, the ratio of peak areas of all C−H groups to peak areas of all groups) can reflect the surface reduction states of soot.[31] The ratio $A_{C-H}/A_{C-H+C=O}$ increased from 0.64 to 0.85 when the fuel/oxygen ratio increased from 0.103 to 0.151 (part B of Figure 6). Stadler and Rossi also found that the oxygen content of soot from a "fuel-lean flame" was higher by a factor of 1.9 than soot from a "fuel-rich flame".[13] These suggest that higher fuel/oxygen ratio will lead to a higher degree of soot surface reduction. Thus, soot with higher fuel/oxygen ratio should have more reactive sites to reduce NO_2 to HONO and NO.

If the ratio of $A_{C-H}/A_{C-H+C=O}$ in the corresponding soot sample represents that in the OC component, the content of OC_R in OC can be estimated through multiplying the $A_{C-H}/A_{C-H+C=O}$ measured by ATR-IR spectra and the OC content measured by TGA. Figure 7 shows the plot of $\gamma_{initial}$, HONO,

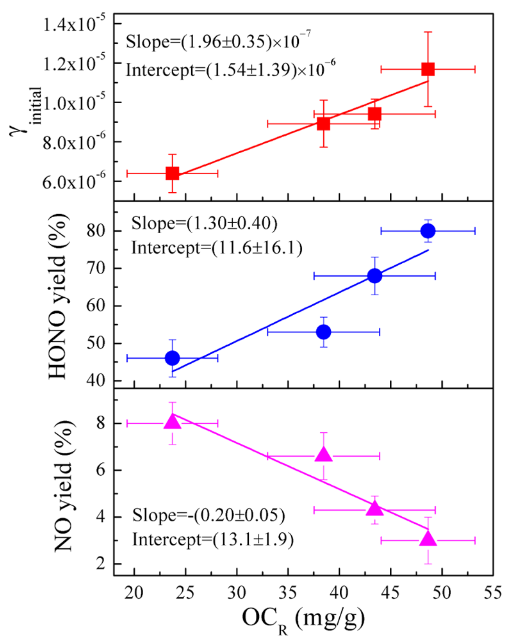

Figure 7. Plot of $\gamma_{initial}$, HONO and NO yield versus OC_R on soot produced at different fuel/oxygen ratios.

and NO yield versus OC_R on soot produced at different fuel/oxygen ratios. The $\gamma_{initial}$ and HONO yield linearly increased with OC_R, while a reversed trend was observed for the NO yield. The slopes for $\gamma_{initial}$, HONO and NO yield were $(1.96 \pm 0.35) \times 10^{-7}$, (1.30 ± 0.40), and $-(0.20 \pm 0.05)$ respectively, which represent the effect of OC_R on the reactivity of soot. The intercept by extrapolation stands for the contribution of EC to NO_2 uptake and HONO and NO formation. The intercept for $\gamma_{initial}$, HONO and NO yield was $(1.54 \pm 1.39) \times 10^{-6}$, (11.6 ± 16.1), and (13.1 ± 1.9), respectively. Moreover, within the uncertainties, these values were close to the $\gamma_{initial}$, and the yields of HONO and NO for the 600 °C-preheated soot. Stadler and Rossi found that no significant decomposition of HONO occurs on the "fuel-rich flame soot", whereas HONO undergoes fast decomposition to NO and N (IV) species on the "fuel-lean flame soot".[13] This was ascribed to more sites with reduction state on fuel-rich flame soot than fuel-lean flame soot.[13] Therefore, the decrease of OC_R with decreasing fuel/oxygen ratio would promote the decomposition of HONO on soot, which may also be the reason of lower HONO yield and higher NO yield on soot with lower fuel/oxygen ratio.

5. ATMOSPHERIC IMPLICATIONS

The atmosphere exhibits an oxidizing nature due to the presence of various oxidizing components such as O_2, OH, O_3, NO_3, N_2O_5, and HNO_3. Once emitted into the atmosphere, soot will undergo aging processes through the uptake of reactive gases.[9−17] This can lead to an increase in the degree of soot surface oxidation, which has been observed during the reaction of soot with 100 ppb O_3 using in situ ART-IR. According to our results, NO_2 uptake coefficients and HONO yields linearly increased with the content of OC with reduced state on soot. Thus, it is reasonable to deduce that oxidizing processes of soot during atmospheric transport will result in a decrease in reactivity of soot toward NO_2, which can reduce the contribution of soot to NO_2 sinks and HONO sources in the atmosphere.

The combustion condition and nature of fuels can significantly modify the content and chemical characteristics of OC on soot. Varied fractions of OC with reduced state may contribute to uncertainties in the reported NO_2 uptake coefficients and HONO yields. In this study, a quantitative relationship between soot reactivity and OC with reduced state was established. If the content of OC with reduced state is known, the contribution of soot to atmospheric NO_2 sinks and HONO sources can be roughly estimated using the linear relationship obtained in this work. Therefore, this study will increase the understanding of soot chemistry in the atmosphere and may also help to assess NO_2 sinks and HONO sources depending on soot compositions.

■ ASSOCIATED CONTENT

Ⓢ Supporting Information

Some environmental details. Diagram of the flow tube reactor. Temporal changes of NO_2, HONO, and NO concentrations in the reaction of NO_2 with soot. The in situ ATR-IR spectra of soot in the reaction with 160 ppb NO_2. This material is available free of charge via the Internet at http://pubs.acs.org.

■ AUTHOR INFORMATION

Corresponding Author

*E-mail: honghe@rcees.ac.cn, phone: +86-10-62849123, fax: +86-10-62923563.

Notes

The authors declare no competing financial interest.

■ ACKNOWLEDGMENTS

This research was financially supported by the National Natural Science Foundation of China (20937004, 20907069, and 50921064). The authors thank the group of M. Ammann

(PSI) as they were the first to point toward the importance of OC on soot chemistry.

REFERENCES

(1) Muckenhuber, H.; Grothe, H. The heterogeneous reaction between soot and NO_2 at elevated temperature. *Carbon* **2006**, *44*, 546−559.

(2) Daly, H. M.; Horn, A. B. Heterogeneous chemistry of toluene, kerosene and diesel soots. *Phys. Chem. Chem. Phys.* **2009**, *11*, 1069−1076.

(3) Jacobson, M. Z. Strong radiative heating due to the mixing state of black carbon in atmospheric aerosols. *Nature* **2001**, *409*, 695−697.

(4) Ackerman, A. S.; Toon, O. B.; Stevens, D. E.; Heymsfield, A. J.; Ramanathan, V.; Welton, E. J. Reduction of tropical cloudiness by soot. *Science* **2000**, *288*, 1042−1047.

(5) Chameides, W. L.; Bergin, M. Soot takes center stage. *Science* **2002**, *297*, 2214−2215.

(6) Menon, S.; Hansen, J.; Nazarenko, L.; Luo, Y. Climate effects of black carbon aerosols in China and India. *Science* **2002**, *297*, 2250−2253.

(7) Gustafsson, Ö.; Kruså, M.; Zencak, Z.; Sheesley, R. J.; Granat, L.; Engström, E.; Praveen, P. S.; Rao, P. S. P.; Leck, C.; Rodhe, H. Brown clouds over South Asia: Biomass or fossil fuel combustion. *Science* **2009**, *323*, 495−498.

(8) Sydbom, A.; Blomberg, A.; Parnia, S.; Stenfors, N.; Sandström, T.; Dahlén, S.-E. Health effects of diesel exhaust emission. *Eur. Respir. J.* **2001**, *17*, 733−746.

(9) Bertram, A. K.; Ivanov, A. V.; Hunter, M.; Molina, L. T.; Molina, M. J. The reaction probability of OH on organic surfaces of tropospheric interest. *J. Phys. Chem. A* **2001**, *105*, 9415−9421.

(10) Lelièvre, S.; Bedjanian, Y.; Pouvesle, N.; Delfau, J.; Vovelle, C.; Bras, G. L. Heterogeneous reaction of ozone with hydrocarbon flame soot. *Phys. Chem. Chem. Phys.* **2004**, *6*, 1181−1191.

(11) McCabe, J.; Abbatt, J. P. D. Heterogeneous loss of gas-phase ozone on *n*-hexane soot surfaces: Similar kinetics to loss on other chemically unsaturated solid surfaces. *J. Phys. Chem. C* **2009**, *113*, 2120−2127.

(12) Arens, F.; Gutzwiller, L.; Baltensperger, U.; Gäggeler, H. W.; Ammann, M. Heterogeneous reaction of NO_2 on diesel soot particles. *Environ. Sci. Technol.* **2001**, *35*, 2191−2199.

(13) Stadler, D.; Rossi, M. J. The reactivity of NO_2 and HONO on flame soot at ambient temperature: The influence of combustion conditions. *Phys. Chem. Chem. Phys.* **2000**, *2*, 5420−5429.

(14) Khalizov, A. F.; Cruz-Quinones, M.; Zhang, R. Heterogeneous reaction of NO_2 on fresh and coated soot surfaces. *J. Phys. Chem. A* **2010**, *114*, 7516−7524.

(15) Saathoff, H.; Naumann, K.-H.; Riemer, N.; Kamm, S.; Möhler, O.; Schurath, U.; Vogel, H.; Vogel, B. The loss of NO_2, HNO_3, NO_3/N_2O_5, and HO_2/$HOONO_2$ on soot aerosol: A chamber and modeling study. *Geophys. Res. Lett.* **2001**, *28* (10), 1957−1960.

(16) Muñozy, M. S. S.; Rossi, M. J. Heterogeneous reactions of HNO_3 with flame soot generated under different combustion conditions. Reaction mechanism and kinetics. *Phys. Chem. Chem. Phys.* **2002**, *4*, 5110−5118.

(17) Kleffmann, J.; Wiesen, P. Heterogeneous conversion of NO_2 and NO on HNO_3 treated soot surfaces: atmospheric implications. *Atmos. Chem. Phys.* **2005**, *5*, 77−83.

(18) Zhang, D.; Zhang, R. Laboratory investigation of heterogeneous interaction of sulfuric acid with soot. *Environ. Sci. Technol.* **2005**, *39*, 5722−5728.

(19) Kleffmann, J.; Becker, K. H.; Lackhoff, M.; Wiesen, P. Heterogeneous conversion of NO_2 on carbonaceous surfaces. *Phys. Chem. Chem. Phys.* **1999**, *1*, 5443−5450.

(20) Lelièvre, S.; Bedjanian, Y.; Laverdet, G.; Bras, G. L. Heterogeneous Reaction of NO_2 with Hydrocarbon Flame Soot. *J. Phys. Chem. A* **2004**, *108*, 10807−10817.

(21) Aubin, D. G.; Abbatt, J. P. D. Interaction of NO_2 with hydrocarbon soot: Focus on HONO yield, surface modification, and mechanism. *J. Phys. Chem. A* **2007**, *111*, 6263−6273.

(22) Ammann, M.; Kalberer, M.; Jost, D. T.; Tobler, L.; Rössler, E.; Piguet, D.; Gäggeler, H. W.; Baltensperger, U. Heterogeneous production of nitrous acid on soot in polluted air masses. *Nature* **1998**, *395*, 157−160.

(23) Prince, A. P.; Wade, J. L.; Grassian, V. H.; Kleiber, P. D.; Young, M. A. Heterogeneous reactions of soot aerosols with nitrogen dioxide and nitric acid: atmospheric chamber and Knudsen cell studies. *Atmos. Environ.* **2002**, *36* (2002), 5729−5740.

(24) Kalberer, M.; Ammann, M.; Gäggeler, H. W.; Baltensperger, U. Adsorption of NO_2 on carbon aerosol particles in the low ppb range. *Atmos. Environ.* **1999**, *33*, 2815−2822.

(25) Kirchner, U.; Scheer, V.; Vogt, R. FTIR spectroscopic investigation of the mechanism and kinetics of the heterogeneous reactions of NO_2 and HNO_3 with soot. *J. Phys. Chem. A* **2000**, *104*, 8908−8915.

(26) Al-Abadleh, H. A.; Grassian, V. H. Heterogeneous reaction of NO_2 on hexane soot: A Knudsen cell and FT-IR study. *J. Phys. Chem. A* **2000**, *104*, 11926−11933.

(27) Akhter, M. S.; Chughtai, A. R.; Smith, D. M. Reaction of hexane soot with NO_2/N_2O_4. *J. Phys. Chem.* **1984**, *88*, 5334−5342.

(28) Smith, D. M.; Welch, W. F.; Graham, S. M.; Chughtai, A. R.; Wicke, B. G.; Grady, K. A. Reaction of nitrogen oxides with black carbon: An FT-IR study. *Appl. Spectrosc.* **1988**, *42*, 674−680.

(29) Smith, D. M.; Chughtai, A. R. The surface structure and reactivity of black carbon. *Colloids Surfaces A* **1995**, *105*, 47−77.

(30) Kolb, C. E.; Cox, R. A.; Abbatt, J. P. D.; Ammann, M.; Davis, E. J.; Donaldson, D. J.; Garrett, B. C.; George, C.; Griffiths, P. T.; Hanson, D. R.; Kulmala, M.; McFiggans, G.; Pöschl, U.; Riipinen, I.; Rossi, M. J.; Rudich, Y.; Wagner, P. E.; Winkler, P. M.; Worsnop, D. R.; O' Dowd, C. D. An overview of current issues in the uptake of atmospheric trace gases by aerosols and clouds. *Atmos. Chem. Phys.* **2010**, *10*, 10561−10605.

(31) Han, C.; Liu, Y.; Liu, C.; Ma, J.; He, H. Influence of combustion conditions on hydrophilic properties and microstructure of flame soot. *J. Phys. Chem. A* **2012**, *116*, 4129−4136.

(32) Monge, M. E.; D́Anna, B.; Mazri, L.; Giroir-Fendler, A.; Ammann, M.; Donaldson, D. J.; George, C. Light changes the atmospheric reactivity of soot. *Proc. Natl. Acad. Sci. U. S. A.* **2010**, *107* (15), 6605−6609.

(33) Cooney, D. O.; Kim, S.; Davis, E. J. Analyses of mass transfer in hemodialyzers for laminar blood flow and homogeneous dialysate. *Chem. Eng. Sci.* **1974**, *29*, 1731−1738.

(34) Murphy, D. M.; Fahey, D. W. Mathematical treatment of the wall loss of a trace species in denuder and catalytic converter tubes. *Anal. Chem.* **1987**, *59*, 2753−2759.

(35) Zelenay, V.; Monge, M. E.; D́Anna, B.; George, C.; Styler, S. A.; Huthwelker, T.; Ammann, M. Increased steady state uptake of ozone on soot due to UV/Vis radiation. *J. Geophys. Res.* **2011**, *116*, D1103.

(36) Nicolas, M.; Ndour, M.; Ka, O.; D́Anna, B.; George, C. Photochemistry of atmospheric dust: Ozone decomposition on illuminated titanium dioxide. *Environ. Sci. Technol.* **2009**, *43*, 7437−7442.

(37) Cain, J. P.; Gassman, P. L.; Wang, H.; Laskin, A. Micro-FTIR study of soot chemical composition—evidence of aliphatic hydrocarbons on nascent soot surfaces. *Phys. Chem. Chem. Phys.* **2010**, *12*, 5206−5218.

(38) Rodríguez-Fortea, A.; Iannuzzi, M. First-principles molecular dynamics study of the heterogeneous reduction of NO_2 on soot surfaces. *J. Phys. Chem. C* **2008**, *112*, 19642−19648.

(39) George, C.; Strekowski, R. S.; Kleffmann, J.; Stemmler, K.; Ammann, M. Photoenhanced uptake of gaseous NO_2 on solid organic compounds: A photochemical source of HONO. *Faraday Discuss.* **2005**, *130*, 195−210.

(40) Pryor, W. A.; Lightsey, J. W. Mechanisms of nitrogen dioxide reactions: Initiation of lipid peroxidation and the production of nitrous acid. *Science* **1981**, *214*, 435−437.

(41) Akhter, M. S.; Chughtai, A. R.; Smith, D. M. the structure of hexane soot I: Spectroscopic studies. *Appl. Spectrosc.* **1985**, *39*, 143−153.

(42) Arens, F.; Gutzwiller, L.; Gäggeler, H. W.; Ammann, M. The reaction of NO_2 with solid anthrarobin (1, 2, 10-trihydroxyanthracene). *Phys. Chem. Chem. Phys.* **2002**, *4*, 3684−3690.
(43) Liu, Y.; Liu, C.; Ma, J.; Ma, Q.; He, H. Structural and hygroscopic changes of soot during heterogeneous reaction with O_3. *Phys. Chem. Chem. Phys.* **2010**, *12*, 10896−10903.